Transport of gases in concrete barriers

Harris, A.W. , Atkinson, A. and Claisse, P.A.

TRANSPORT OF GASES IN CONCRETE BARRIERS

A.W. Harris, A. Atkinson and P.A. Claisse*

Materials Chemistry Department, Materials and Manufacturing Technology Division,
AEA Industrial Technology, Harwell Laboratory, Didcot, Oxon. OX11 0RA, United Kingdom.

* Present address; Department of Civil Engineering, The University,
Dundee DD1 4HN, United Kingdom.

Abstract

The performance of the cementitious materials within a radioactive waste repository as a physical barrier to the migration of radionuclides depends on the maintenance of the integrity of the barrier. Potentially, this can be compromised by physical damage to the barrier caused by pressurisation as gas is generated within the repository. The maintenance of chemical homogeneity within the material used for backfilling the repository may also be compromised as a consequence of gas pressurisation through the formation of additional cracks and the reaction of cementitious materials with gases such as carbon dioxide. Consequently, the migration of gas within repository construction materials may be a significant parameter in both the design of a repository and the provision of a safety case for disposal.

The migration of hydrogen, helium, methane, argon and carbon dioxide have been studied for materials selected to be typical of repository structural concretes and grouts that are being considered for backfilling and waste encapsulation. The apparent permeability of these materials to gas has been shown to be dependent on gas type and average pressure in the structural concrete due to the effects of Knudsen flow at pressures of the order of 100 kPa. This is not observed in the grouts due to the significantly greater pore size. The permeability coefficients for the grouts are several orders of magnitude greater than those of the concrete. Gas migration is strongly influenced by the degree of water saturation of the materials. The presence of interfaces within the materials results in an increase in permeability at higher degrees of water saturation.

A simple model has been developed to simulate the effects of gas pressurisation. The tangential hoop stress at the surface of a void is calculated and comparison with the expected tensile strength of the materials is used to assess the potential for cracking. The backfill grouts seem to have sufficient permeability to disperse gas without crack formation.

1 Introduction

The strategy adopted by many countries for the disposal of low and intermediate level radioactive wastes requires an engineered repository placed at considerable depth underground. Typically, such a repository will lie below the water table and hence will become water saturated relatively soon after the cessation of operations and closure. The majority of disposal strategies, including that adopted by UK Nirex Ltd., the body responsible for low and intermediate level radioactive waste in the United Kingdom, require that the waste packages be surrounded by a backfilling material. The most commonly adopted types of backfilling material are based on either hydraulic cements or clay materials such as bentonite [1]. Much of the remainder of the engineered structure of a repository may also be constructed of materials based on hydraulic cements; in particular structural concretes. The current disposal strategy in the United Kingdom envisages a cement-based material for backfilling. Consequently, the properties of such cementitious materials are important both in the design of the repository and in the safety assessment.

Gas will be generated within a radioactive waste repository by several mechanisms. The principal such mechanisms are the corrosion of steel reinforcement and containers (to generate hydrogen), the degradation of organic components in the waste (to yield carbon dioxide and methane) and the radiolysis of water (yielding hydrogen and oxygen). The majority of the gas generated will be either hydrogen, methane or carbon dioxide. The local pressure within the repository will rise above the ambient hydrostatic pressure to a value determined in the steady state by the relative rates of gas generation and release due to migration out of the immediate repository structure into the geological environment. A sufficient rise in internal pressure may result in stresses large enough to damage the repository structure and hence may compromise the containment strategy. In addition, gas-driven water flow, in the form of bulk water or bubbles, has the potential to short-circuit the repository containment by carrying contaminated water direct to the geological environment without prior conditioning of the water to high pH. Thus, data for, and the understanding of, the migration of gases within potential repository construction materials are required in order that the likelihood of such an eventuality can be determined and, if required, allowed for in the repository design.

Cementitious materials may be utilised for three main purposes in the United Kingdom repository; structural components, backfilling of the repository vaults and the encapsulation of materials within the actual waste packages. The materials selected for study in this work were chosen to be typical of those which may be adopted for each of these three applications. The structural concretes studied were relatively conventional materials based on either sulphate resistant Portland cement (SRPC) or a mixture of ordinary Portland cement (OPC) and pulverised fuel ash (PFA), together with both fine and coarse limestone aggregates. The waste encapsulation material was represented by a grout based on a 1:9 mixture of OPC and blast furnace slag (BFS) containing no aggregate.

The cementitious backfilling material requires a high porosity both to provide a high capacity for the sorption of radionuclides and to readily condition the chemistry of the mobile water in the repository. Two materials of this type, differing in composition and compressive strength, have

been studied in this work. They are referred to in the text as preliminary backfill grout and reference backfill grout. The actual mix designs of these materials are regarded as commercially sensitive and cannot be specified further.

This study has investigated the migration of a range of gases in the five different materials detailed above by both bulk flow and diffusion. The sensitivity of gas migration to a range of variables, including water content and average pressure in the range 0.1 to 7.5 MPa, has been investigated. The effect on gas migration of interfaces necessarily present within the repository due to the process of construction has been assessed for concrete containing reinforcement and backfill grout containing a construction joint. A discussion of previously reported experimental techniques for the measurement of gas migration and the results obtained is provided to allow comparison with the data obtained from the present work. The implications of the results for the behaviour of gases within a radioactive waste repository are considered using a simple model of stress generation and cracking based on the behaviour of a hollow spherical body.

2 Background

2.1 Mechanisms of Gas Migration

The migration of gases within porous media is the subject of an extensive literature and has been reviewed on several occasions [2-5]. The fundamental mechanisms of gas migration are flow due to an imposed pressure gradient and flow due to a composition gradient. These are termed bulk, or permeable, and diffusive migration respectively.

The steady-state viscous flow of a fluid in a capillary under an imposed pressure gradient at sufficiently low Reynolds numbers (Re<2100) is governed by the Hagen-Poiseuille law [2, 3]. In a real porous medium the Hagen-Poiseuille law must be modified to allow for the convolutions of the pore structure, resulting in Darcy's equation for the bulk, or viscous, flow of an effectively incompressible fluid such as water [2, 3, 6];

$$\frac{dV}{dt} = \frac{kA}{\mu}\frac{dp}{dx} \qquad ....(1)$$

where dV/dt is the volumetric flow rate, k the permeability coefficient, A the cross-sectional area of the medium perpendicular to the direction of flow, μ the fluid viscosity and dp/dx the applied pressure gradient. The permeability coefficient is considered to be a property specific to the porous material and hence should be independent of the both the properties of the fluid and the specific transport mechanisms. In a highly compressible fluid, that is a gas, the pressure gradient cannot be considered to be independent of position in a material and, even in a steady state, the volumetric flow rate is significantly different at every point in the medium. Under steady-state conditions, the molecular flux must be conserved throughout the medium and consequently Darcy's equation can be re-cast in terms of the molecular flow rate, dn/dt [2];

$$\frac{dn}{dt} = \frac{kA\bar{p}}{\mu RT}\frac{\Delta p}{l} \qquad ....(2)$$

where p is the average pressure in the medium and Δp the pressure difference imposed across specimen thickness l.

It has been frequently observed that the gas permeability of a porous medium is dependent on the gas pressure. Hence, the permeability coefficient for a gas in a particular medium will generally differ from that measured for an incompressible fluid. This effect was noted by Klinkenberg from investigations of migration of gas in oil reservoirs [7]. An empirical equation was proposed to describe these observations;

$$k = k_{\infty}(1 - b/p) \qquad ....(3)$$

where k is the gas permeability coefficient measured at average pressure p, k_{∞} the gas permeability coefficient which would be observed at infinite pressure and b a constant termed the Klinkenberg constant. Hence, the measured gas permeability coefficient decreases with increasing average pressure. The infinite pressure permeability coefficient should be equal to the permeability coefficient for an incompressible fluid. Klinkenberg also observed that the value of the constant was dependent on the water permeability coefficient.

The Klinkenberg effect is due to an additional contribution to the assumed viscous flow from Knudsen or "slip" flow at low pressures [2, 3, 9]. Hence, at some particular range of pressure the mechanism of gas flow will be transitional between viscous and Knudsen flows. The Knudsen flow regime becomes significant when the mean free path of the gas is of the same order as or greater than the size of the capillary or pore in which the gas is flowing. The consequent reduction in the interaction between the gas molecules and the capillary wall results in a non-zero flow adjacent to the capillary walls, increasing the overall flow relative to the purely viscous flow regime. The mean free path is inversely dependent on pressure and hence the contribution from Knudsen flow in a particular medium is reduced at higher pressures.

The migration of a species under a composition gradient, as opposed to a pressure gradient, is characterised by a material dependent parameter known as the diffusion coefficient. This coefficient is determined by Fick's laws of diffusion [10];

$$\frac{\partial n}{\partial t} = -D\frac{\partial c}{\partial x} \qquad ....(4a)$$

$$\frac{\partial c}{\partial t} = D\frac{\partial^2 c}{\partial x^2} \qquad ....(4b)$$

where c is the concentration and D the diffusion coefficient. In an unconfined system, the rate of

diffusion of a gas is determined by the molecular velocity and hence, at a given temperature, the rate of diffusion is inversely dependent on the square root of the molecular mass. In a confined system, such as a porous medium, the inter-diffusion of two gases at a constant pressure results in a shift of the centre of mass of the system because the lighter gas diffuses more rapidly. Consequently, the migration of gases at constant pressure must be effectively described as the sum of a diffusive flow and a non-segregative bulk flow [2]. Alternatively, if the pressures are not constrained to remain equal to the initial pressure, the differing diffusive flow rates result in an imbalance in the pressures and a pressure difference arises. This is known as the Kirkendall effect [3, 11]. The resulting bulk flow exactly counter-balances the difference in diffusive flows and the rate of change in composition of each gas is equal. Hence, only a single diffusion coefficient can be determined, the inter-diffusion coefficient for the pair of gases utilised.

The movement of molecules during the diffusion of a gas in a porous medium can occur by both the normal, "viscous" type flow and by Knudsen flow [12]. Consequently, gas diffusion coefficients may be dependent on the pressure in similar manner to permeability coefficients discussed above.

The migration of gases within the pore structure of the cementitious materials intended for use in repository construction is likely to be complicated by the presence of pore water. Under fully water saturated conditions the pores will be effectively blocked and, for lower gas pressure gradients, the only plausible mechanism of gas migration will be the aqueous phase diffusion of gas molecules which have become dissolved in the water. It is currently not known whether the conditions within a repository will result in completely water-saturated material or whether some air will be trapped. At a sufficient excess internal pressure difference the gas should be able expel a proportion of the pore water from the porosity of even fully-saturated material, allowing migration in what is effectively a small volume fraction of open porosity. Under such conditions, the migration will in reality be a two-phase flow. In the current work this complication is ignored and the gas migration treated as a simple single phase situation.

The production of gas within a radioactive waste repository subsequent to closure and re-saturation by water will result in an increase in pressure above the prevailing hydrostatic pressure. Consequently, it is expected that gas migration will be primarily driven by excess pressure. Some degree of migration will occur by the solution-diffusion mechanism. It is not expected that gaseous diffusion will be of concern in the post-closure situation although it may be of relevance during the operating period.

2.2 Experimental Measurements of Gas Migration
2.2.1 Gas Permeability of Cementitious Materials

Measurements of the permeability of cementitious materials to fluids have been extensively reported. However, experimental measurements of the permeability of such materials to gases in particular are less widely available. Previously reported data are generally concerned with the development and validation of experimental techniques intended for determining gas permeability for model cement pastes [13] or structural concretes [8, 14-18] and as a parameter to be correlated

with the durability of structural concretes, often as an *in situ* technique [19].

The techniques employed for the measurement of gas permeability differ substantially in detail but are all based on the determination of the flow rate of a gas under an applied pressure gradient. The most common technique utilises a membrane-type arrangement with a specimen of material separating two gas reservoirs at different pressures. The flow rate into the lower pressure reservoir is monitored with a flow meter, generally of the bubble-type [8, 14, 16-18, 20]. Typical applied pressures utilised lie in the range 0.2 to 1 MPa, resulting in pressure gradients of the order of 1 to 20 MPa m^{-1}. The determination of the permeability from the measured flow rate is relatively straightforward for this "membrane" technique. An alternative technique utilises the decay of a known pressure due to the flow of gas to determine the permeability [15, 19]. Martin describes the implementation of such an experimental technique but this method of data analysis utilised provides only a qualitative indication of permeability [15].

The actual gas permeability coefficients for cementitious materials cover a wide range, depending on the composition and condition of the material. This range is typically about 10^{-21} to 10^{-15} m^2. The lower permeability coefficients are those measured for water-saturated materials where the flow rates for such materials are often too low to be measured in the membrane technique. Hence, the majority of reported measurements of permeability are for dried materials.

The intrinsic permeability coefficient of a porous material is generally considered to be determined by the properties of the material and hence should be independent of the permeating fluid. However, at the pressures typically utilised for gas permeability measurements, the gas permeability coefficient is generally found to be significantly in excess of that for water. Bamforth has found that the gas permeability lies between 5 and 80 times that for water in a variety of concretes [8]. This phenomenon is attributed to the additional contribution to the flow of a gas provided by Knudsen flow. Bamforth compared his experimental data for gas and water permeabilities with the relationship proposed by Klinkenberg for oil reservoir sands [7]. He observed a similar dependence of the Klinkenberg constant on the water permeability coefficient for the cementitious materials although the experimental data indicated a slightly different relationship to that observed for the sands [8].

Daimon *et al* measured the permeability coefficients of vacuum-dried OPC-sand mortars using hydrogen and nitrogen as the migrating gases [21]. An expression for the measured permeability coefficient in terms of the relative contributions of viscous and Knudsen flow was derived and applied to the experimental data. Both the viscous and Knudsen contributions were found to decrease with curing time. The change in the viscous contribution was significantly greater, indicating a relative increase in the contribution from Knudsen flow as the pore structure became finer with increased curing. The viscous and Knudsen contributions for hydrogen were respectively greater and less than those for nitrogen.

The relative contribution of Knudsen flow to the overall rate of gas migration is dependent on the pore size of the porous medium, and hence on both the composition and conditioning of a cementitious material, and on the mean free path of the permeating gas. Consequently, the simple comparison of gas permeability coefficients for different materials at a single pressure is of limited

utility in a more fundamental study of gas migration. However, much of the published data on gas permeation is limited to such a comparison due to the requirements of the particular authors for simple tests related to, for example, concrete durability [16, 17, 19].

Grube and Lawrence have determined the repeatability of membrane permeability measurements on dried concretes and find that, for a single specimen, repeated measurements give a coefficient of variability of 3-4 % [17]. Similarly, Cabrera and Lynsdale measured variabilities of between 0.3 and 1.5 % for a single specimen [16]. In contrast, the coefficient of variability for measurements on different specimens of the same material is considerably greater; measured values vary from 7.5 % [16] to a range of 15-24 % [17]. Such values are typical of the inter-specimen variability observed for measurements of other mass-transport parameters for cementitious materials [22].

The gas permeability of concrete has been found to vary substantially with the age of the material. Cabrera and Lynsdale found a decrease in the permeability coefficents by factors of around 20 in a period of 90 days after casting for several different mortars [16]. The final permeabilities of dried materials were typically $2x10^{-17}$ m^2. Grube and Lawrence have reported a similar decrease in oxygen permeability with curing time for a range of different concretes examined in a study performed in several laboratories. The absolute values of the gas permeability coefficients showed considerable variability between the different laboratories participating in the measurements. The range of measured values was about $2x10^{-18}$ to $2x10^{-16}$ m^2 [18]. This range of permeability coefficient is typical of the values obtained for dried structural materials [8, 13].

The gas permeability of water-saturated material has not been widely reported due to experimental difficulties. The behaviour of a 3:1 BFS/OPC grout has been reported after drying to various weight losses [23]. The measured permeability was strongly correlated with the weight loss. Specimens with a nominal 90 % water saturation (specimens dried to give 10 % of the weight loss observed on full drying) gave a permeability coefficient of about 10^{-18} m^2 whilst fully saturated material had a permeability coefficient below the limit of resolution of the technique; 10^{-20} m^2. Chou Chen and Katz report that the permeability coefficient for methane in wet concrete is several hundred times smaller than that measured in dry material [20]. The appropriate permeability coefficients are $8.3x10^{-17}$ and $4.7x10^{-14}$ m^2 respectively. The water permeability coefficient for the wet material was substantially lower than that for methane even in the wet material.

It is apparent that the majority of published data on gas permeability are determined for either hardened cement pastes or structural materials in a dry condition. Consequently, there is little available data relevant to the type of high porosity material currently envisaged as the Nirex repository backfill.

2.2.2 Gaseous Phase Diffusion in Cementitious Materials

The diffusion of gases in porous materials has been extensively measured but published data directly relevant to cementitious materials are scarce. Daimon *et al* [20] measured the inter-diffusion of hydrogen and nitrogen in vacuum-dried OPC-sand mortars at constant pressure.

The diffusion coefficients obtained were dependent on curing time and initial water-cement ratio. After 28 days, the diffusion coefficients were 4.8×10^{-7} and 1.9×10^{-7} m^2s^{-1} for water-cement ratios of 0.65 and 0.5 respectively. The diffusion coefficients showed a significant decrease with increasing average pressure, indicative of the contribution of Knudsen flow at low pressures.

Lawrence [24] measured the inter-diffusion of nitrogen and oxygen in a range of concretes as a function of various parameters. The experiments were performed at a constant pressure using an oxygen sensor to determine the concentration within the flowing nitrogen gas. Specimens were cured at 55% relative humidity and allowed to surface dry prior to measurement. Subsequent drying caused changes in the diffusion coefficients until constant values were reached. The diffusion coefficients were strongly dependent on curing time and water-cement ratio, as observed by Daimon $et\ al$ [21]. The measured values lay in the approximate range 2×10^{-9} to 2×10^{-7} m^2s^{-1}. The values were quite well correlated with measured water permeability coefficients. Tuutti [25] has reported a series of measurements of the diffusion coefficient for oxygen in concrete based on Portland cement both with and without the addition of BFS. The unmodified material was studied under a variety of relative humidity conditions and the diffusion coefficient was found to decrease from about 7×10^{-8} m^2s^{-1} in the dry condition to about 3×10^{-10} m^2s^{-1} after conditioning at 100 % relative humidity. The slag-modified materials were found to have diffusion coefficients which were a factor of 2 to 5 times lower than the unmodified material under the same conditions.

The diffusion of radon gas through concrete structures has also been studied. In general, experiments were performed on actual structures and hence the condition of the concrete was not well defined. It is assumed that it was relatively dry. Measured diffusion coefficients lay in the range 7.5×10^{-7} to 1.9×10^{-7} m^2s^{-1} [26, 27]. The diffusion of methane in wet and dry structural concretes has been investigated by Chou Chen and Katz [20]. The diffusion coefficients for dry material were in the range 3.6×10^{-8} to 3.1×10^{-7} m^2s^{-1} whilst those for wet material lay between 1.3×10^{-9} and 1.8×10^{-8} m^2s^{-1}. The values for wet material are somewhat greater than those reported by Tuutti for 100 % relative humidity [25]. This may indicate that the "wet" material does not represent full water saturation.

The above measured values for diffusion coefficients are all similar in magnitude and hence the approximate range of values for the diffusion coefficient for dry material can be given as about 10^{-9} to 10^{-7} m^2s^{-1}.

2.2.3 Aqueous Phase Diffusion of Dissolved Gases

Page and Lambert directly measured the aqueous diffusion of oxygen derived from the gaseous phase in hardened cement pastes using an electrochemical technique [30]. The measured diffusion coefficients were dependent on the water cement ratio of the material and were in the range 1.3×10^{-12} to 2.2×10^{-12} m^2s^{-1} at 25 °C. The activation energy for the diffusion was typically half that for chloride ions.

The diffusion of chloride ions derived from ionic compounds has been reported for migration in hardened cement pastes [22, 28, 29]. Whilst there is no direct evidence that the aqueous phase migration of chlorine gas occurs exclusively via the diffusion of chloride ions, it is likely that some

ions will be produced on dissolution and hence chloride ion diffusion data has some relevance to the consideration of gas migration. The measured chloride ion diffusion coefficients were of the order of 10^{-11} m^2s^{-1}.

3 Experimental Method

3.1 Experimental Materials

3.1.1 Manufacture and Physical Properties

The experimental materials used in this study were prepared at either Sir Robert McAlpine Ltd. or by Taywood Engineering Ltd.. The ratios of water to hydraulic binder and aggregate to binder and the total cement contents for the concretes are given in Table 1. Commercial considerations mean that the compositions of the backfill grouts cannot be given. The materials were mixed in pan or shear mixers as appropriate and vibrated into moulds. The SRPC and PFA/OPC-concretes and the BFS/OPC-grout were cured for 24 hours at 20 °C prior to de-moulding then cured underwater at ambient temperature for 28 days. All materials were subsequently stored underwater at ambient temperature until required for use. The resulting compressive strengths and densities of all the experimental materials are given in Table 2.

The pore structures of all materials except the SRPC-concrete were investigated using mercury intrusion porosimetry (MIP) using a Carlo Erba Strumentazione Porosimeter 2000 with a maximum operating pressure of 200 MPa. The sample of the PFA/OPC-concrete was prepared by taking a number of 10 mm cores from a larger specimen and breaking these up and mixing to ensure a representative sample was achieved. Simple cores were used for the remaining materials. The porosity and the average pore radius were obtained from the MIP and these data are given in Table 2. In addition, the porosity was calculated from the weight loss on drying, given in Table 3, using the measured density of water-saturated material from Table 2. The discrepencies between the two methods of obtaining the porosity may be due either to the MIP failing to intrude fine pores or the drying causing the loss of some water of hydration. It is likely that the MIP data are the more accurate.

The MIP results revealed that the PFA/OPC-concrete and the BFS/OPC-grout have relatively narrow and symmetrical pore size distributions in the range 5 to 50 nm. In contrast, the preliminary and reference backfill grouts have broad pore size distributions ranging from 5 nm to greater than 1 μm. These distributions are quite strongly biassed towards the larger pore sizes as shown by the average radii given in Table 2.

3.1.2 Specimen Conditioning

The specimens were conditioned prior to use in a controlled humidity atmosphere to establish a known water content. Three different humidities were selected; zero, 75 % and 100 % relative humidity. The SRPC-concrete was used in the dry condition only. The zero humidity, dry specimens were dried for 24 hours at 100 °C then stored in a sealed container containing silica gel dessicant. The remaining specimens were placed directly into sealed containers. The 75 % and 100 % relative humidities were achieved by placing a quantity of saturated sodium chloride

solution or demineralised water respectively into the containers. The degree of water saturation was determined by monitoring weight loss during conditioning. The fractional weight losses incurred by conditioning, compared to the initial weight in a surface dry condition, are given in Table 3. The data in Table 3 confirm that that the grouts have substantial porosity and show that both the preliminary and reference grouts lose water even during conditioning at 100 % relative humidity.

Analysis of the experimental data from the gas transport experiments was carried out using a numerical model of the gas migration process, as described below, and requires the measurement of the "gas-accessible" volume for each type of material and condition. This was measured by placing appropriate specimens into a sealed chamber at a known pressure and subsequently venting the gas into an additonal, known volume. The resulting pressure drop, combined with the volumes of the system and the specimen, can be used to calculate the volume of porosity accessible by gas. This method has the advantage that the specimens are used in an intact, conditioned state and the measured porosity is directly associated with gas migration. The measured porosities obtained using this technique are given in Table 3.

The gas accessible porosity values for the backfill grouts are not significantly different from those obtained from weight loss measurements, as given in Table 3. The gas accessible porosity values were subject to some inaccuracy due to limitations in the measurements of the volumes. However, it appears from the comparison of the data in Table 3 that the PFA/OPC-concrete and BFS/OPC-grout have significantly lower gas accessible porosities than is indicated by other measurement techniques.

3.1.3 Specimens Containing Interfaces

The influence of artefacts introduced by the construction process was assessed using specimens containing reinforcement bars and construction joints. It is expected that the reinforcement will be confined to the structural concrete. The backfill grout will be placed in a series of separate pours and hence the construction joints will primarily influence gas migration in the backfill. The effect of interfaces on gas migration was investigated using specimens conditioned at both zero and 100 % relative humidity.

Specimens of the PFA/OPC-concrete were cast into moulds containing a section of reinforcing mesh oriented vertically in a cylindrical mould. The mix design and curing conditions utilised were identical to those discussed above. The mesh consisted of 4 mm diameter bars spaced at 50 mm intervals. The cylinders were sectioned between the horizontal members of the mesh to produce specimens containing two bars perpendicular to the flat faces of the slices. The arrangement of the reinforcement bars in the cylinder is illustrated in Figure 1. The interface between the reinforcement and the concrete was parallel to the direction of gas migration.

Construction joints were produced in specimens of the preliminary backfill grout. Previously cast cylinders, cured identically to those described previously, were split approximately in half in the direction perpendicular to the flat faces and replaced in moulds prior to casting additional material of the same mix design as the original specimens. A further monolithic specimen was

prepared from the additional material to act as a control. The specimens were subsequently cured at ambient temperature for at least 28 days. Sectioning produced specimens with the construction joint oriented parallel to the direction of gas migration.

3.2 Gas Diffusion Measurements

3.2.1 Experimental Apparatus

The general form of the experimental apparatus employed in these measurements is illustrated schematically in Figure 2. The experimental apparatus also allowed the sampling of a fixed volume of the gas from one side of the cell. Specimens were in the form of 100 mm discs approximately 20 mm in thickness mounted into a perspex holder using a cold-setting urethane compound (Devcon Flexane-94). Previous work has shown that this material provides an effective barrier to both aqueous and gaseous species and subsequent experiments have shown that integrity of the seal is maintained for periods in excess of a month [22].

The inter-diffusion of hydrogen and argon was measured for the SRPC-concrete in the dry condition using two different experimental techniques. The inter-diffusion coefficient was obtained directly by monitoring changes in gas composition and indirectly by the measurement of the transient pressure gradient induced during the diffusion process.

3.2.2 Gas Composition Monitoring

The diffusion of hydrogen into an argon carrier gas through a membrane of the SRPC-concrete was monitored by removing samples of the hydrogen-contaminated argon at regular intervals. The sampled volume was replaced with pure argon. The gas composition was measured using gas chromatography, with a sensitivity of better than 0.1 %. The volume of gas analysed was 75 cm^3, which, when losses during sampling are included, represents approximately half of the total volume of the carrier gas. Replacement of a significant fraction of the "contaminated" carrier gas by pure argon has the effect of increasing the concentration gradient across the specimen and lowering the the hydrogen concentration at the onset of the subsequent sampling period. This effect had to be allowed for in the analysis of the experimental data.

Samples were taken every five minutes in the period up to an elapsed time of 35 minutes and every 10 minutes thereafter. The process of of removing and replacing the sample cylinders took approximately two minutes. This time is a significant fraction of the total time elapsed between sampling events and results in some systematic error in the results.

3.2.3 Diffusion-induced Pressure Transients

During the measurement of gas composition changes it was observed that the transient pressure differences induced by the Kirkendall effect were of significant magnitude. These pressure transients were measured and analysed to determine an estimated inter-diffusion coefficient for hydrogen and argon as described below. The measurements were made using initial pressures of 100, 125, 155 and 175 kPa. It was assumed that the average pressure in the system remained equal to the initial pressure throughout the course of an experiment.

The inter-diffusion coefficient was estimated in the following way. The kinetic energies of the gases are equal and therefore the velocity of hydrogen molecules will be $\sqrt{40}/2$ times that of argon, due to the difference in molecular mass. Consequently, the unconstrained diffusion rate of hydrogen should be approximately 4.5 times that of argon. The effect of this difference in diffusion rates will be balanced by bulk flow under the induced pressure gradient. The required bulk molecular flow rate will be equal to half the difference between the diffusive flow rates, that is (4.5-1)/2, or 1.75, times the argon diffusive flow rate. The overall effective interdiffusion rate will be equal to the average of the two diffusion rates, that is (4.5+1)/2, or 2.75, times the argon diffusive flow rate. Hence, the ratio of the bulk flow rate to the diffusive flow rate will be 1.75/2.75 or 0.64.

The actual bulk molecular flow rate can be calculated from the Darcy equation, suitably modified to allow for the effect of the compressibility of the gas, and the ideal gas approximation as discussed above. The diffusive flow rate can be derived from Fick's first law. The concentration of the gas molecules in the reservoir initially containing argon is also given by the ideal gas approximation and combining this with Fick's law for diffusion under a time invariant concentration gradient gives;

$$\frac{dn}{dt} = \frac{DA}{l}\frac{p}{RT} \qquad ....(5)$$

where dn/dt is now the diffusive molecular flow rate, D the inter diffusion coefficient and, in this case, p the pressure in the reservoir initially containing hydrogen. The above equation assumes that the absolute amount of gas exchange between the reservoirs is relatively small and consequently that the hydrogen concentration is effectively zero in the argon reservoir. The ratio of the bulk and diffusive molecular flow rates is, as argued above, equal to 0.64. Hence, combining the equations for bulk and diffusive molecular flow gives;

$$D = \frac{k\bar{p}\,\Delta p}{0.64\,\mu p} \qquad ....(6)$$

This equation can be used to calculate the inter-diffusion coefficient. The derivation assumes that the peak in the pressure transient corresponds to steady-state diffusion.

3.3 Gas Permeability Measurements

3.3.1 Experimental Apparatus

The flow of gas under an imposed pressure gradient was measured by monitoring the decay of a pressure difference across a membrane of the material with elapsed time. This technique bears some similarities to that developed by Martin [15] except that in the present work the pressure was monitored on both sides of the membrane. The apparatus is illustrated schematically in Figure 2.

Experimental measurements were carried out using a variety of gases. The permeability of the dry SRPC-concrete was measured using hydrogen and argon whilst that of the BFS/OPC and backfilling grouts and the flawed specimens was measured using helium and argon. The influence of gas type on gas migration was more fully investigated for the PFA/OPC-concrete using five different gases; hydrogen, helium, methane, argon and carbon dioxide.

The experimental apparatus was designed to allow the maintenance of a constant humidity atmosphere adjacent to the specimen during an experiment. This was achieved by placing either desiccant, salt solution or pure water into the cell along with the specimen.

Measurement cells were constructed for operation at both low (0-200 kPa) and high (0-10 MPa) applied pressures. The low pressure cells were identical to those utilised in the diffusion experiments. The higher pressure experiments were performed either with or without triaxial confinement of the specimens. In particular, it was found that triaxial stressing of the high porosity preliminary backfill grout caused a substantial permanent reduction in the volume of the specimens and some experimental error may have occurred. The specimen thickness was dependent on the measurement cell used. In the case of the triaxial cell specimens approximately 10 cm thick were used whilst in the other cells the specimen thickness was approximately 2 cm. The construction of the low pressure cells gave a reduction in the area of specimen exposed in the lower pressure reservoir compared to that exposed in the high pressure reservoir. Where necessary, a correction by a factor of 1.13 has been applied to the data to allow for this effect.

Two variations on the basic experiment were performed. In the first, both reservoirs shown in Figure 2 were isolated and the pressures allowed to relax to an equilibrium level. Such experiments allowed measurements to be made at an approximately constant average pressure. In contrast, measurements were also performed with a continuously varying average pressure by holding one reservoir at a constant applied pressure. In both cases, the range of average pressure values was determined by the initial conditions and the volumes of the two reservoirs.

The permeability measurements were made at a range of different average pressures. Constant average pressures of 100 kPa and 1.5, 7, 15, 22 and 72 MPa were used in the measurements on the PFA/OPC-concrete whilst experiments on the grouts were constrained to a maximum average pressure of about 25 MPa to avoid specimen damage. The varying average pressure experiments were performed in two pressure ranges; 0 to 200 kPa and 0 to 3 MPa, denoted low and high pressure ranges respectively.

Between one and ten measurements were carried out for each set of conditions. The data generally exhibited very little variability between different runs on an individual specimen. It was considered that a measured permeability coefficient represented the sum of the permeability coefficient of the material and any additional contribution from short-circuit pathways such as cracks or incomplete sealing between specimen and container. Hence, it was not possible to obtain a measured permeability coefficient below the true permeability coefficient for the material. The best value of the permeability coefficient for a material was taken to be the lowest value obtained.

The elapsed times required for the completion of a particular experiment was determined by the material being studied. These varied from about 10 seconds, in the case of dry preliminary

backfill grout, to greater than one month for some of the materials in the 100 % relative humidity condition. The limit of accuracy of the experiments was ultimately controlled by the quality of the seals achieved in the measurement cells, both between the two reservoirs and to atmosphere. The effective lower and upper limits of resolution of the experimental apparatus were estimated as 10^{-21} and 10^{-14} m^2 respectively. Since the permeability coefficients are based on calculations of the rate of change of pressure, any experimental errors, such leaks between reservoirs or to atmosphere, will result in an over-estimate of the permeability coefficient. The presence of leaks to atmosphere can be detected in the closed system mode by checking for conservation of the total mass of gas as it flows from one reservoir to the other.

3.3.2 Analysis of Experimental Data

The flow of a single gas between the two reservoirs in the apparatus will be such that the pressure difference is reduced and eventually eliminated. The flow of a fluid in a homogeneous porous medium under a pressure gradient is governed by the Darcy equation given previously. The volumetric flow rate can be related to the molecular flow rate using the ideal gas approximation and the resulting version of the equation integrated across the whole specimen to give an expression for the molecular flow rate in terms of the applied pressures on either side of the membrane. The variation in pressure in one reservoir, in this instance that at the lower pressure, can be determined from this expression by the further application of the ideal gas approximation;

$$\frac{dp_1}{dt} = \frac{kA}{2\mu l V_1}\left[(p_2)^2 - (p_1)^2\right] \qquad ....(7)$$

where dp_1/dt is the rate of pressure change in the low pressure reservoir, V_1 the volume of that reservoir and p_1 and p_2 the pressures in the low and high pressure reservoirs respectively. In a closed experiment, the change in pressure in the high pressure reservoir can be calculated from that measured in the lower pressure reservoir and hence p_2 obtained from p_1. Substituting for p_2 and integrating with respect to pressure and time gives an expression for the variation of pressure in the low pressure reservoir with time;

$$\frac{[(V'^2 - 1)\,p_1 - (V'+1)\,(\beta + V'\alpha)]\,[(\beta - \alpha)\,V' + \alpha - \beta]}{[(V'^2 - 1)\,p_1 - (V' - 1)\,(\beta + V'\alpha)]\,[(\beta + \alpha)\,V' + \alpha + \beta]}$$
$$= \exp\left[\frac{kA}{\mu l V_1}\,(\beta + V'\alpha)\,t\right] \qquad ....(8)$$

where V' is the ratio of the reservoir volumes (V_1/V_2) and α and β are the initial low and high pressures respectively. If the higher pressure is held constant, the effective value of V_2 is infinite and the ratio V' is zero. Applying this constraint to the equation above allows the determination of

permeability coefficient from the experiments with variable average pressure. The variation in the pressure in the higher pressure reservoir can be obtained using an analogous method. This derivation predicts the exponential relaxation of an applied pressure difference with time which was observed experimentally by Martin [15].

The analytical solution for gas pressure variation given above assumes that steady state flow has been established. That is that the quantity of gas exiting the specimen into the lower pressure reservoir is equal to that entering the specimen from the higher pressure reservoir. For a compressible fluid in a medium with finite porosity this is not strictly true. Hence, the analytical solution is only applicable to materials where the error caused by the assumption of zero porosity is not significant. The errors become large in specimens of high porosity subject to a large pressure difference. In order that the all the experimental data could be analysed, a numerical model of the variation in pressure with time was developed using a finite-element method. The value of permeability coefficient obtained from the analytical solution was input as a starting value for the numerical calculation. Subsequently, the numerical model was run to produce a simulated data set of pressure versus time from which a new permeability coefficient was calculated using the analytical solution. This process was repeated until the simulated data set achieved a satisfactory match to the experimental data.

The permeability coefficients quoted in Section 4 below were obtained using this numerical method to extract the permeability coefficient from both constant and varying average pressure experiments. The analytical solution alone was used to calculate the infinite pressure permeability coefficients and Klinkenberg constants from the varying average pressure experiments. It is expected that these data will not be as accurate as those derived from the numerical solution.

The completion of an experiment is indicated by the achievement of a uniform pressure throughout the experimental apparatus. For materials with a low porosity, this pressure is equal to a volume-weighted average of the initial pressures in the two reservoirs. However, if the porosity is high, there is significant gas volume contained in the specimen and the final average pressure must include a contribution from the gas in the pore volume. If the flow is in steady state, the average pressure, p, in the pore volume is not the linear average of the two initial pressures, due to the compressibility of the gas, but is given by;

$$\bar{p} = \frac{2}{3} \frac{(p_1)^3 - (p_2)^3}{(p_1)^2 - (p_2)^2} \qquad ....(9)$$

The overall average pressure can then be calculated using this value for the pressure in the pore structure and weighting according to the volume of the porosity. In some experiments, the volume of the porosity can be as much as half of the total volume. The assumption that the average pressure in the porosity is a linear average can lead in such circumstances to under-estimation of the expected final pressure by over 10 %.

4 Results

4.1 Diffusion in SRPC-concrete

4.1.1 Gas Composition Monitoring

The measured variation in the hydrogen concentration as a function of time within the argon reservoir is shown in Figure 3. Each sampling event required that approximately half of the hydrogen was removed from the system and consequently the concentration was reduced after each sampling event. Figure 3 is constructed on the assumption that exactly half of the volume of the gas was removed during each sampling event. In the period between 10 and 25 minutes elapsed time, it appeared that the hydrogen removed was being completely replaced by the diffusive flow during the subsequent sampling period. This allowed the effective molecular flow rate to be estimated as 2×10^{-7} mol s^{-1}. The estimated hydrogen-argon inter-diffusion coefficient based on this flow rate is approximately 10^{-8} m^{2}s^{-1}.

4.1.2 Diffusion-induced Pressure Transients

The variation in the pressure difference between the two reservoirs due to the Kirkendall effect at an average pressure of 125 kPa is shown in Figure 4. The calculation of the inter-diffusion coefficient using the method given previously requires the permeability coefficient for the material. The appropriate values of the argon permeability coefficient (discussed below) and the calculated diffusion coefficient for each average pressure are given in Table 4. It is apparent from the table that there is no systematic dependence of the diffusion coefficient on the average pressure at the pressures used in these experiments and hence the hydrogen-argon inter-diffusion coefficient is estimated as 3×10^{-8} m^{2}s^{-1} for dry SRPC-concrete.

4.2 Gas Permeability of Structural Concrete

4.2.1 Gas Migration at Constant Average Pressure

A typical pressure difference relaxation curve for a specimen of the PFA/OPC-concrete is shown in Figure 5. The final average pressure is predicted by the equation given above. Figure 6 shows a comparison of the gas permeability coefficients for the PFA/OPC-concrete obtained using hydrogen, helium, methane, argon and carbon dioxide as the migrating gases. Measurements were made on material conditioned at 0, 75% and 100% relative humidity. All experiments were performed at an average pressure of 100 kPa. Data for the 100 % relative humidity conditioned specimen are only available for helium and argon. If the Klinkenberg relationship is applicable to this data, the measured permeabilities at constant pressure will depend on the mean free path for each gas. The mean free path, λ, can be calculated in a number of ways, the equation used here is;

$$\lambda = \frac{2.02 \, \eta}{\sqrt{p \rho}} \qquad \ldots(10)$$

Where η is the viscosity, p the average pressure and ρ the density. The mean free paths for the

gases used at a pressure of 100 kPa and a temperature of 25 °C are given in Table 5. The variation in the permeability coefficient with the type of gas for both the dry and 75 % relative humidity conditioned specimen at 100 kPa, given in Figure 6, is correlated with the mean free path of the gas given in Table 5. Linear regression on the two data sets gave correlations of $r^2 = 0.92$ and 0.75 for the dry and 75% relative humidity conditioned specimens respectively. The intercept as the mean free path tends to zero determined by linear regression gives the value of the infinite pressure permeability which equate with that in the Klinkenberg equation, since a mean free path of zero corresponds to a value of the Klinkenberg constant of zero. The infinite pressure permeability coefficients derived in this way are 1.3×10^{-17} m^2 for dry material and 2×10^{-20} m^2 for that conditioned at 75 % relative humidity.

4.2.2 Variation in Gas Permeability with Average Pressure

The values of the permeability coefficient of the SRPC-concrete in the dry condition for hydrogen and argon migration at a range of approximately constant average pressures between 0 and 150 kPa is shown in Figure 7. The data have been corrected by a factor of 1.13 to allow for the differing areas of the specimen exposed in the high and low pressure reservoirs as a result of the seal geometry. It is clear that the permeability coefficient is inversely dependent on average pressure. The permeability coefficient for hydrogen exceeds that for argon in the pressure range investigated. This is consistent with the observations made above and can be attributed to the increasing effect of Knudsen flow at lower pressures and the longer mean free path of hydrogen for a given pressure.

The Klinkenberg equation can be fitted to the data, as illustrated in Figure 7. The infinite pressure permeability coefficients thus determined are 3.6×10^{-18} and 4.0×10^{-18} m^2 from the hydrogen and argon data respectively. These values are close enough to be considered equal, within experimental error. The calculated values of the Klinkenberg constant are 6.6×10^5 Pa for hydrogen and 4.2×10^5 Pa for argon.

The dependence of the gas permeability for argon migration in the PFA/OPC-concrete (conditioned at zero humidity) on the average pressure is shown in Figure 8. Data are included for experiments performed at both constant and varying average pressures. The range of data obtained at each pressure is illustrated. It is apparent that the permeability coefficient decreases as the average pressure is increased. Plotting the best estimate permeability coefficient for the set of experiments performed at, approximately, a particular value of the average pressure against the reciprocal of average pressure indicated that the Klinkenberg relationship is probably applicable, although the correlation obtained was not strong ($r^2 = 0.78$). Linear regression gave the infinite pressure permeability as 2.0×10^{-17} m^2 and the Klinkenberg constant as 190 kPa.

The change in permeability with average pressure shown in Figure 8 is most significant at low average pressures. The results of a series of measurements performed with the average pressure varying between 0 and 200 kPa in PFA/OPC-concrete conditioned at zero relative humidity, using each of the five different gases, are given in Table 5. There is a possible correlation between the Klinkenberg constant and the mean free path for each gas, calculated using

the equation above, at a pressure of 100 kPa and a temperature of 25 °C ($r^2 = 0.60$).

The infinite pressure permeability coefficient should be a constant value, independent of the type of gas. The variation in the infinite pressure permeability coefficient with gas type is not strongly correlated with the mean free path ($r^2 = 0.50$) and it is assumed that the differences between the values shown in Table 5 are due to experimental error. The mean value of the infinite pressure permeability coefficient is $(3.7\pm0.6) \times 10^{-17}$ m^2. This value is reasonably consistent with the values of 1.3×10^{-17} and 2.0×10^{-17} m^2 determined above.

The results of the measurements carried out with a varying average pressure of argon on the PFA/OPC-concrete conditioned at 100 % relative humidity implied an infinite pressure permeability of $(7.6\pm2.3) \times 10^{-17}$ m^2. Comparison of this value with those given in Figure 6 indicate that the former must be subject to error as the permeability is apparently 3 orders of magnitude greater when measured in the varying average pressure experiment. The varying average pressure experiments were performed using higher pressure differences, up to 3 MPa. It is postulated that the high applied pressures gave rise to mechanical failure in the specimens when used in the non-triaxial high pressure cell. Consequently, the data for PFA/OPC-concrete in the 100% relative humidity condition have been omitted from Table 7.

4.3 Gas Permeability of Grouts

4.3.1 Gas Migration at Constant Average Pressure

Table 6 details the measured permeability coefficients for the migration of helium and argon at an average pressure of 100 kPa in all of the experimental materials in both the dry and 100 % relative humidity conditioned states. The data for the PFA/OPC-concrete are included for comparison. In some of the materials in the dry state, in particular the two types of backfill grout, the gas migration was so rapid that only variable average pressure experiments could be performed. In these cases the permeability coefficients for a constant average pressure of 100 kPa were calculated from the available data for varying average pressure, discussed below, using the Klinkenberg equation.

4.3.2 Variation in Gas Permeability with Average Pressure

The infinite pressure permeabilities for all of the experimental materials are shown in Table 7 for migration at low pressure in materials conditioned at 0 and 100 % relative humidity, with the exception of the value for the PFA/OPC-concrete in the 100 % relative humidity condition. It has been assumed that the infinite pressure permeability is a constant for all gases and hence the infinite pressure permeability coefficients given are the average of the data for all gases studied in each material. Figure 9 illustrates the fit of the Klinkenberg equation to the variation in the measured permeability coefficient for the BFS/OPC-grout for average pressures in the range 0 to 100 kPa.

Table 8 gives the measured values of the Klinkenberg constant for all the experimental materials in the dry condition for both low and high average pressures. Where the table shows that the Klinkenberg constant is within experimental error of zero or negative, the change in permeability with pressure over the pressure range investigated was very small. A negative value

may be the result of a systematic error in the data analysis when the change in permeability coefficient is small. In such circumstances, it must be assumed that the permeability coefficient is constant with average pressure and equal to the infinite pressure permeability coefficient.

The Klinkenberg constants for the materials in the 100 % relative humidity conditioned state were not measured for all materials and pressure ranges. When the values were measured, using high average pressures, in the range 0 to 3 MPa, the Klinkenberg constants were found to be negative or not significantly different from zero for all materials. The data were considered to indicate that there was little or no change in the permeability coefficient for average pressures in the high pressure range.

4.4 The Effect of Interfaces on Gas Permeability

4.4.1 Influence of Reinforcement on Gas Migration

The permeability coefficients for a constant average pressure of 100 kPa and the infinite pressure permeability coefficients for both the dry and 100 % relative humidity conditioned specimens are given in Table 9. These data can be directly compared with the data for pristine, that is unreinforced, PFA/OPC-concrete given in Tables 6 and 7.

The presence of the reinforcement bars appeared to increase the permeability coefficient of dry material (measured at a constant average pressure of 100 kPa) by a factor of between three and four. There was no significant difference between pristine and reinforced material for the 100 % relative humidity condition at a constant average pressure of 100 kPa. However, at a constant average pressure of about 1.6 MPa, the permeability coefficients for helium and argon were increased to 2×10^{-19} and 1×10^{-19} m² respectively. This represents an increase by about an order of magnitude compared to the data at obtained at 100 kPa. This increase in permeability with average pressure is not observed for the pristine material and must be attributed to the influence of the reinforcement.

The infinite pressure permeability coefficient for dry material is approximately a factor of five greater in the reinforced concrete. Comparable data for pristine material in the 100 % relative humidity condition is not available.

4.4.2 Influence of Construction Joints on Gas Migration

The experimental results obtained for the preliminary backfill grout containing a construction joint are given in Table 9. No data were obtained at constant average pressure in dry material as the extremely high permeability made experiments too rapid. The control specimen gave a 100 kPa argon permeability coefficient of 6.3×10^{-16} m² for material in the 100 % relative humidity condition. The infinite pressure permeability coefficients for the control specimen were 2.3×10^{-13} and 4.6×10^{-16} m² for the dry and 100 % relative humidity conditions respectively. These data are significantly greater than those obtained for the normal specimens of the grout, given in Tables 6 and 7. It is apparent that the batch of grout used in the preparation of the construction joints is not consistent with the other specimens of this material.

The construction joint increased the 100 kPa permeability of 100 % relative humidity

conditioned material by a factor of three compared to the control specimen and a factor of 70 compared to the pristine material. The infinite pressure permeability was equal to that of the control specimen for the dry condition and was approximately an order of magnitude greater for the 100 % relative humidity condition.

4.5 Variability in the Measurements

The contribution to experimental error arising from inter-specimen variability is mainly due to the variation in the number of short-circuit pathways in different specimens of the same material. In addition, some irreproducibility may occur between individual experimental runs on the same specimen and from differences in the intrinsic permeability coefficients of individual specimens of the same material. The total variability in the measurements of the permeability coefficient for a particular material under a fixed set of conditions can be quantified by the coefficient of variability of the data. This is equal to the ratio of the standard deviation to the mean for the data, usually expressed as a percentage.

The permeability coefficient measurements made at a constant average pressure of 100 kPa, summarised in Figure 6 and Table 6, generally exhibited overall coefficients of variability of between 10 and 40 %. The reproducibility of repeated measurements on an individual specimen was generally of the order of a few percent. In contrast, previous measurements of the aqueous diffusion coefficients for similar cementitious materials indicated a variability between repeated measurements of the same property of a single specimen of between about 10 and 30 % [16, 17, 22]. Hence, the measurement of gas permeability using this experimental technique seems to be inherently reproducible.

In contrast, the measured infinite pressure permeability coefficients, given in Table 7, had coefficients of variability of between about 30 and 200 %. The large variability in the infinite pressure permeability coefficients is due to the error produced when the Klinkenberg equation is fitted to data which exhibit a very small change in permeability over the pressure range investigated. This is particularly true of the backfill grouts.

5 Discussion
5.1 Gas Migration in Structural Concretes
5.1.1 Gas Diffusion in Structural Concretes

The best value of the hydrogen-argon inter-diffusion coefficient for the SRPC-concrete in a dry condition, 3×10^{-8} m^2s^{-1}, is similar in magnitude to the values obtained by other workers and discussed previously. The gas migration parameters measured for the other materials indicate that the parameters for the high porosity backfilling grouts exceed those for the structural materials by an order of magnitude or more. Consequently, the value of the diffusion coefficient for the SRPC-concrete represents a lower limit to the diffusion coefficients for the other materials, in particular the backfilling grouts. Gas migration by diffusion will only be significant during the operating phase of the repository. In these circumstances, the gases generated within the backfilled structure may migrate by inter-diffusion with gases within the air in open, operational vaults.

5.1.2 Bulk Gas Flow in Dry Material

The experimental data shown in Figure 6 demonstrate that the permeability coefficient for the PFA/OPC-concrete measured at a constant average pressure of 100 kPa is dependent on the mean free path of the gas. Experiments conducted with a varying average pressure show that the permeability coefficient for a particular gas in both the SRPC- and PFA/OPC-concretes decreases with increasing average pressure, as shown by the data in Table 5 and Figure 7. This variation is also demonstrated by the compilation of the data for argon migration in dry PFA/OPC-concrete shown in Figure 8. These observations are consistent with previous observations by other workers which demonstrate that the gas permeability of structural concretes is influenced by Knudsen flow at lower pressures [8].

The data for the SRPC-concrete, shown in Figure 7, demonstrate that this material exhibits a significantly lower permeability than does the PFA/OPC-concrete. This is at variance with the general expectation that the mass transport characteristics of a PFA-modified material will be lower than those of an unmodified cement [22]. The infinite pressure permeability coefficient given in Table 7 for the SRPC-concrete is an order of magnitude lower than that given for the PFA/OPC-concrete. The measured fractional porosities of the two materials, given in Table 2, are similar. The observed difference in performance may be the result of differing degrees of damage to the pore structures of the two materials during drying.

The contribution of Knudsen flow to the flow of a given gas is characterised by the Knudsen number; the ratio of the mean free path to the radius of the pores in which the gas is flowing. A Knudsen number significantly greater than unity indicates that Knudsen flow will be important. The mean free path is dependent on the nature of migrating gas, as shown above. Consequently, the contribution from Knudsen flow at a given pressure will depend on the gas flowing, as shown by the data in Figure 6. The average pore radius for the PFA/OPC-concrete, given in Table 2, is 0.011 μm whilst the mean free path at 100 kPa and 25 °C varies between 0.070 and 0.305 μm for the gases used in these experiments. Hence, the Knudsen numbers are in the range 6 to 28 and a significant contribution from Knudsen flow at 100 kPa would be expected.

The data shown in Figure 8 demonstrate that the change in the argon permeability coefficient of the PFA/OPC-concrete for an increase in the average pressure from 100 kPa to 7.5 MPa is a decrease by about a factor of 2.5. Comparison of the infinite pressure permeability coefficients for dry material given in Table 5 for the different gases with the permeability coefficients obtained at a constant average pressure of 100 kPa given in Figure 6 also indicates that the permeability decreases by at most a factor of two as the pressure is increased over this range. The majority of this decrease occurs in the 0 to 1 MPa pressure range, as shown in Figure 8.

5.1.3 Bulk Gas Flow in Water-saturated Material

The behaviour of the PFA/OPC-concrete in the partially or fully water saturated condition is qualitatively similar to that in a dry condition. Figures 5 and 6 demonstrate that the permeability coefficient is dependent on the type of gas for concrete conditioned at 75 % relative humidity, although the measured permeability coefficients are significantly lower than those of dry material.

The reduction in the measured permeability coefficient for material conditioned at high relative humidities must be due to the effective blocking of pores which remained filled with water after conditioning. The relationship between the radius of the largest filled pore, r_p, and relative humidity, H, is given by the Kelvin equation [3];

$$-\ln (H) = \frac{2\sigma}{r_p} \frac{V}{RT} \qquad ....(11)$$

where σ and V are the surface tension and molar volume of water respectively. A relative humidity of 75 % gives a maximum filled pore radius of about 4 nm whilst at a relative humidity of 100 % all pores should be filled with water. Hence, at 75 % relative humidity the majority of the porosity should be available for gas migration. The reduction in the permeability coefficient for 75 % relative humidity conditioned materials apparent in the experimental results hence indicates that gas migration is significantly influenced by the finer porosity and that much of the pore volume may not form interconnected networks with constrictions larger than 4 nm.

The material conditioned at 100 % relative humidity demonstrated a further decrease in the permeability coefficient. The Kelvin equation predicts that all porosity is water-filled for this condition and hence a reduction is expected. However, the only mechanism available for gas migration in material that is fully water-saturated will be solution-diffusion, where dissolved gas molecules diffuse in the pore solution. Using a solubility of 9×10^{-4} M and a diffusion coefficient of 2×10^{-12} m^2s^{-1} [30], an equivalent permeability coefficient of about 10^{-23} m^2 is obtained. This value is significantly less than that obtained for helium migration in the PFA/OPC-concrete, 7×10^{-20} m^2, and it must be concluded that either there was leak across the specimen or that some interconnected porosity remains open in the specimens conditioned at 100 % relative humidity.

5.2 Gas Migration in Grouts

Table 6 shows that the permeability coefficients at 100 kPa for the three different grouts in the dry condition are of similar magnitude and are an order of magnitude or more greater than those measured for the PFA/OPC-concrete. The permeability coefficients for the grouts are decreased by two or three orders of magnitude for the 100 % relative humidity conditioned specimens compared to the dry materials. The permeability coefficients for the BFS/OPC-grout in the 100 % relative humidity conditioned state is substantially lower than those of the other grouts and is comparable in magnitude to that of the structural concrete.

Comparison of the data obtained using helium and argon as the migrating gases in dry materials shows that there is no significant dependence on gas type for the preliminary backfill grout. Hence, there is apparently little or no Knudsen flow occurring at 100 kPa. Some dependence on gas type is exhibited by the BFS/OPC- and reference backfill grouts. The observed variation in behaviour must be due to the differences in pore sizes between the grouts.

Comparison of the permeability coefficients extrapolated to infinite pressure, given in Table

7, with those obtained at 100 kPa average pressure, (Table 6) indicates that there is no consistent relationship between the two. This demonstrates that the permeability coefficients of these materials are not strongly dependent on average pressure at pressures of 100 kPa and above. The values of the Klinkenberg constants for these materials were extracted from the data. However, the results were found to be extremely variable and some values were negative, indicating an increase in the permeability coefficient with increasing average pressure. Hence, the permeability coefficients for the high porosity grouts can be considered to be approximately constant over the range of average pressures studied here.

The difference between the behaviour of the grouts and that of the PFA/OPC-concrete must be due to differences in the pore structures of the materials. Table 2 shows that the average pore sizes of the preliminary and reference backfill grouts are 0.7 and 0.4 μm respectively. These values are such that the Knudsen numbers for the two materials will be significantly less than unity at an average pressure of 100 kPa and hence no significant contribution from Knudsen flow would be expected in these materials at this, or greater, pressure.

5.3 Comparison with Water Permeability Coefficients

Since the viscous flow of fluids is governed by the Darcy equation, the permeability coefficient should be equal for all fluids. The flow of gases is complicated by the Klinkenberg effect and compressibility, but the infinite pressure permeability coefficients for dry material should be equal to the permeability coefficients for liquids such as water [2, 3, 8]. The data for material conditioned at 100 % relative humidity cannot be directly compared to that for water flow.

The water permeability coefficients for both the SRPC- and PFA/OPC-concretes have been shown to be less than about 10^{-21} m^2 [33]. Table 6 indicates that the infinite pressure permeability coefficients for the concretes are more then four orders of magnitude greater than this. Although, the water permeability measurements were complicated by the continued hydration of the materials it is unlikely that the difference can be explained by this effect.

The water permeability coefficient of the preliminary backfill grout has been measured as about 4×10^{-16} m^2 [31]. This value is approximately two orders of magnitude lower than the infinite pressure permeability coefficient of the dry grout given in Table 7. In contrast, the water permeability of the reference backfill grout, at 2×10^{-16} m^2 [32], is close to the infinite pressure permeability coefficient. No water permeability data are available for the BFS/OPC-grout.

The data discussed above demonstrate completely different relationships between water and gas permeability coefficients. Only the reference backfill grout shows the close agreement between the two data expected initially. The reasons for these differences in the behaviour of the materials are uncertain, and may reflect differences in pore structure under dry and wet conditions, that is the presence of water not only fills pore space but changes its characteristics.

5.4 Interaction between Gas and Water in Cementitious Materials

Comparison of the permeability coefficients obtained for the experimental materials in the dry and 100 % relative humidity conditioned states demonstrates that the influence of water within the

pore structure of cementitious materials is crucial in determining gas migration rates. The comparison between the effective permeability coefficient for the solution-diffusion migration mechanism and the measured permeability coefficients demonstrates that none of the experimental materials can be considered to be fully water saturated under any of the experimental conditions in this study.

As discussed above, the only mechanism available for gas migration in fully water-saturated material is solution-diffusion. The equivalent permeability coefficient for solution-diffusion, about 10^{-23} m^2, is significantly lower than the lowest permeability coefficients measured for any of the 100 % relative humidity conditioned materials. Hence it appears that the gas migration observed in this study may differ significantly from that expected for the truly water-saturated condition.

The application of a pressure difference to a water saturated porous material will result in the expulsion of water from pores which exceed a particular size. The expulsion of a fluid from a capillary requires the application of an excess pressure denoted the capillary pressure. The capillary pressure, p, for a pore of radius r, assuming an angle of contact between the fluid and the capillary wall of 90°, is given by [2];

$$p = \frac{2\sigma}{r} \qquad ....(12)$$

where σ is the surface tension, equal to 0.073 Nm^{-1} for water. The approximate capillary pressures for the average pore radius of both the PFA/OPC-concrete and the BFS/OPC-grout are 13 MPa whilst those for preliminary and reference backfill grouts are 210 and 320 kPa respectively.

In the low pressure experiments, the maximum applied pressure is 200 kPa. This pressure can expel water from pores of the order of 0.7 μm. The MIP results for the two backfill grouts show that both materials exhibit a significant volume of porosity with pore radii above this value. Hence, water expulsion may occur in the 100 % relative humidity conditioned specimens even in the low pressure experiments. Measurements made on the backfill grouts using higher applied pressures may exhibit significant water expulsion effects. This would result in measured permeability coefficients in excess of that expected for fully saturated material based on the solution-diffusion model of gas migration. In addition, the increased expulsion of water at higher pressures may give an increase in permeability with applied pressure.

The above discussion assumes that the average pore radius obtained from the MIP measurements is the maximum pore size available. This is unlikely to be true and, although the pore size distributions of the high-porosity grouts are substantially skewed towards the larger pore sizes, there will be significant porosity with radii in excess of the average values. The experimental results appear to demonstrate that the migration of gas is significantly affected by the presence of these larger pores.

Similar effects would be expected for the PFA/OPC-concrete and the BFS/OPC-grout.

However, the finer pore structure would mitigate the effect and hence the measured permeability coefficients for 100 % relative humidity conditioned material should be closer to the value predicted by the solution-diffusion model. This is demonstrated by the comparison between the measured permeability coefficients for these materials and those measured for the backfill grouts.

The weight losses measured during conditioning at 100 % relative humidity for both the preliminary and reference backfill grouts indicate that full water saturation may not be achieved prior to the commencement of the experiments. It is possible that the water within the larger pores in these materials is draining under the influence of gravity. Thus, the data obtained for 100 % relative humidity conditioned specimens may not be representative of the behaviour of fully water saturated material.

The retention of water within a capillary is governed by the balance between the capillary pressure and the gravitational force exerted by the weight of the water. Consequently, water will only be retained in pores of a given radius if the pore length does not exceed a particular value. This length can be calculated by equating the capillary pressure to the hydrostatic pressure of a column of water;

$$h = \frac{2\sigma}{r\rho g} \qquad ....(13)$$

where h is the maximum pore length which can remain water filled and g the acceleration due to gravity. The maximum pore lengths are 21 and 32 m for the preliminary and reference backfill grout average pore radii respectively. Since the specimen thicknesses are only a few centimetres, it is apparent that the weight loss cannot be explained by gravitational draining.

If the movement of water under the influence of gravity is occurring, despite the argument above, it may provide an additional means whereby the migration of gas within a repository could occur. In particular, the movement of water may allow a consequent migration of gas as a "bubble".

6 The Effects of Stress Generation in Cementitious Materials

6.1 Model of Cracking in Cementitious Materials

6.1.1 Simple Analytical Model of Crack Generation

The effects of the stress generated by gas pressurisation have been studied using a simple model of a spherical gas source in spherical repository. The model is illustrated schematically in Figure 10. The ultimate effect of stress will be a failure of the backfill resulting in the formation of a crack. If the region of gas generation shown in Figure 10 is considered to be a void then backfill failure at the void surface will occur if the tangential hoop stress exceeds the tensile strength of the backfill. Hence, in the model the crucial stress for determining the failure of the material is considered to be the tangential hoop stress at the surface of the void.

The relationship between the tangential hoop strain at a particular radius, r, denoted e_θ, and

the radial and tangential hoop stresses acting at that position is given by [34];

$$e_\theta = \frac{1}{E} \{(1-v)S_\theta - vS_r\} \quad ....(14)$$

where S_r and S_θ are the radial and tangential hoop stresses respectively and v and E the Poisson's ratio and Young's modulus for the backfill material. The tangential hoop strain at a particular radius is also equal to the ratio of the radial displacement at that point to the radius.

Analytical solutions exist for the tangential hoop stress and radial stress at a given radius for a spherical pressure vessel [34]. The repository model can be considered to be equivalent to such a situation and hence the equations for the stresses at radius r and the radial displacement of the inner surface, y, are;

$$S_r = \frac{-\Delta p\ R^3\ (\zeta^3 - r^3)}{r^3\ (\zeta^3 - R^3)} \quad ....(15)$$

$$S_\theta = \frac{\Delta p\ R^3\ (\zeta^3 + 2r^3)}{2r^3\ (\zeta^3 - R^3)} \quad ....(16)$$

$$y = \frac{\Delta p}{E}\left[\frac{(1-v)\ (\zeta^3 + 2R^3)}{2(\zeta^3 - R^3)} + v\right] \quad ....(17)$$

where Δp is the excess pressure in the void (compared to the hydrostatic pressure in the medium surrounding the repository) and R and ζ the radii of the void and the repository respectively. The above equations are derived for the particular case where the porosity of the repository construction material is zero.

The radial displacement of the inner surface of the repository, that is the surface of the void, can be derived from Equations 15 to 17 by putting the radius at which the stress is to be calculated, r, equal to the void radius, R. It can be shown that if the outer radius, ζ, is more than an order of magnitude greater than the void radius, Equations 15 to 17 can be further simplified by assuming that the outer radius is effectively infinite. The dimensions of a repository are likely to be of the order of tens of metres whilst the voids will be of the order of a few tens of centimetres. Hence, the assumption that the outer radius is effectively infinite is reasonable for is this model of stress generation. The radial displacement of the void surface, y_v, is then given by;

$$y_v = \frac{\Delta p\ R\ (1+v)}{2E} \quad ....(18)$$

Dividing the radial displacement of the void surface, given by Equation 18, by the radius of the void and equating to the tangential hoop strain given in Equation 14 produces an expression for the

Page 26

tangential hoop stress at the void surface;

$$S_\theta = \frac{1}{(1-v)} \left[\frac{\Delta p\,(1+v)}{2} + vS_r \right] \quad \dots (19)$$

For the zero porosity case, the radial stress can be derived from the equation given previously. This gives a radial stress equal in magnitude to the excess pressure in the void, although negative in sign. The tangential hoop stress obtained from Equation 19 is then equal to half the excess pressure. This is a standard result for a pressure vessel.

The effect of the porosity of the backfill material has been included into the model by modifying the value utilised for the radial stress.

$$S_r = -(1-\epsilon)\,\Delta p \quad \dots (20)$$

where ϵ is the fractional porosity of the material. This approach is rather simplistic, but, as discussed below, it can be shown to be a good approximation for the conditions applicable to the behaviour of a repository. Substituting the equation for the radial stress into the expression for the tangential hoop stress given in Equation 19 gives;

$$S_\theta = \frac{\Delta p}{2} \left[1 + \frac{2v\epsilon}{(1-v)} \right] \quad \dots (21)$$

This expression can be used to calculate the hoop stress using appropriate parameters. The backfill is considered to fail if the calculated stress exceeds the tensile strength of the material.

6.1.2 Numerical Solution for Non-zero Porosities

The analytical solution for the tangential hoop stress at the surface of the void is an approximation which takes limited account of the effect of the backfill porosity. The validity of this approximation was tested using a numerical approach.

The numerical model explicitly considered the inward and outward forces acting on a spherical shell within the backfill, centred on the gas-generating inclusion, with an inner radius r and an outer radius r+dr. The inward force, F_i, and outward force, F_o, are respectively;

$$F_i = 4\pi r^2 \,(\epsilon dp - S_r) \quad \dots (22)$$

$$F_o = 4\pi (r+dr)^2 \left[\frac{2S_\theta dr}{r} - (S_r + dS_r) \right] \quad \text{....(23)}$$

where dp is the pressure difference across the shell, and dS_r the change in radial stress across the shell. In a stable situation these forces will be equal. Equating the two forces gives;

$$dS_r = \frac{S_r r^2}{(r+dr)^2 - 1} + \frac{2S_\theta dr}{r} - \varepsilon dp \quad \text{....(24)}$$

The radial strain, e_r, is equal to the rate of change of radial displacement with radius, that is strain is given by dy/dr. The standard definition of radial strain gives;

$$e_r = \frac{1}{E} \{S_r - 2\nu S_\theta\} \quad \text{....(25)}$$

Equations 22 to 25 were used to determine the radial displacement of the void surface by iterating until a constant value of radial stress was obtained. The boundary conditions imposed on the procedure were that the radial stress at the void surface was equal to the excess pressure, modified by porosity, and that at infinite radius was zero. The radial displacement was then used to calculate the tangential hoop stress.

The numerical solution was used to obtain the hoop stress at the void surface and the value compared to that obtained using the analytical approximation. It was found that the difference between the two solutions was negligible and the analytical equation, combined with a description of the pressurisation of the void given in Section 6.1.3, was adopted for subsequent calculations.

6.1.3 Pressurisation of the Void

Gas is considered to be generated within the void in the material. The excess pressure produced by the gas generation will depend on the rate at which the gas can flow through the material. The volumetric flow rate within the backfill material at a radius r, denoted dV/dt, is determined by the pressure at that position, p(r), and the gas generation rate Q, measured at the hydrostatic pressure p;

$$\frac{dV}{dt} = \frac{Qp}{p(r)} \quad \text{....(26)}$$

The volumetric flow rate is is also given by the Darcy equation (Equation 1), provided that the value of the pressure gradient utilised is that at the appropriate radius. Combining Equations 1 and 26 and rearranging gives an equation for the pressure gradient at radius r;

$$\frac{dp}{dr} = \frac{\mu Qp}{Akp(r)} \qquad ....(27)$$

where A is the area of the spherical shell of radius r. This expression can be integrated between the void radius, R, and the outer radius of the repository, ζ. This gives an expression for the pressure produced in the void, p_v;

$$p_v^2 - p^2 = \left[\frac{1}{R} - \frac{1}{\zeta}\right]\frac{Q\mu p}{2\pi k} \qquad ....(28)$$

If it is assumed that the outer radius is effectively infinite, Equation 28 can be simplified and rearranged to yield an equation for the difference between the pressure in the void and the hydrostatic pressure, the excess pressure, Δp, utilised in previous equations;

$$\Delta p = \frac{Q\mu p}{2\pi k R (p_v + p)} \qquad ....(29)$$

substituting the expression for Δp given in Equation 29 into Equation 21 gives an expression for the tangential hoop stress generated at the void surface by a given void pressure, p_v;

$$S_\theta = \frac{1 + 2v\varepsilon}{1-v} \frac{Q\mu p}{4\pi k R (p_v + p)} \qquad ....(30)$$

This equation is used to calculate the tangential hoop stresses in the discussion in Section 6.2.

6.2 Sensitivity to Material Properties and Conditions
6.2.1 Basis of Calculations

The sensitivity of the tangential hoop stress, calculated using the analytical approximation given in Equation 30, to the material parameters required by the model was investigated. The effect of a particular parameter was assessed by fixing all remaining parameters at typical values and varying the parameter of concern over an appropriate range. The typical parameters were selected to reasonably approximate the reference backfill grout in a water saturated condition. It is apparent from the analytical approximation that the calculated stress in this model is independent of the Young's modulus of the material. The gas viscosity was assumed to be equal to that of argon at a value of 2.2×10^{-5} Pas.

The tangential hoop stress at the void surface calculated from the typical values of the model parameters is 238 kPa. The compressive strength of the reference backfill grout is 6.0 MPa. If the tensile strength is assumed to be one tenth of the compressive strength, that is 600 kPa, then the

tensile strength is not exceeded by the hoop stress for the typical conditions and the reference backfill grout will not crack.

6.2.2 Gas Generation Rate

The anticipated maximum gas generation rate is approximately one repository volume of gas per year, measured at standard temperature and pressure. The model is intended to represent the venting of gas from a single waste drum with an approximate volume of 1 m^3. Hence, the typical value of the generation rate was taken to be 1 m^3 per year at standard temperature and pressure. The range of generation rates was specified as 0 to 5 m^3 per year. The variation in stress with gas generation rate is shown in Figure 11. The stress is increased as the gas generation is increased.

6.2.3 Hydrostatic Pressure

The majority of current radioactive waste disposal strategies envisage the placement of a repository at a depth of up to 1000 m below ground level. This indicates a potential range of hydrostatic pressures of between 100 kPa and 10 MPa if the repository is fully saturated by the groundwater. Figure 11 demonstrates that the stress is inversely dependent on the hydrostatic pressure and hence the lower pressure of 100 kPa was adopted as the typical value to represent a plausible worst case. The reduction in stress with increasing hydrostatic pressure is attributed to the compressibility of the gas. As the pressure increases the volumetric flow rate is decreased. This behaviour implies that a repository will be more susceptible to gas generated cracking before re-saturation by groundwater as the effective hydrostatic pressure will be lower.

6.2.4 Fractional Porosity

The data given in Table 2 indicate a range of fractional porosities of between about 0.1 and 0.6 for the experimental materials. The relationship between the measured values of fractional porosity and that available for gas flow is not known. The typical value was taken as 0.5, close to the values given for the backfill grouts in Table 2. The analytical solution demonstrates that gas generated stress is linearly dependent on the fractional porosity of the material, assuming constant permeability. The stress increases by a factor of 0.5 as the porosity is varied between zero and unity. The effect of porosity on the stress may not be adequately modelled by the analytical approximation and the dependence of stress on porosity may not be as simple as indicated here.

6.2.5 Void Radius

The model is intended to simulate that effects of gas vented from waste drums. It is expected that any vent will be of the order of the size of the drum; approximately 0 to 1 m in dimension. The typical value of 0.05 m was selected to represent a vent of 10 cm diameter. Figure 11 demonstrates that the stress generated at the surface of the void is strongly dependent on the void radius. The requirement for a void dimension is a limitation in the overall model and Figure 11 shows that the value of the void radius is crucial in determining the level of stress.

6.2.6 Poisson's Ratio

The expected value of the Poisson's ratio for an ideal material is 0.5. The values for real materials tend to be between about 0.2 and 0.4 and hence a range of 0 to 0.5 was investigated. The typical value was taken to be 0.2. The stress increased by a factor of two as the Poisson's ratio was varied between 0 and 0.5. Variation in this parameter is not of primary importance in determining the stress.

6.2.7 Permeability Coefficient

As has been discussed previously, the repository is likely to become water saturated at some stage after closure and hence the gas permeability will be influenced by the presence of water. Figure 11 demonstrates that the stress is strongly dependent on permeability for permeability coefficients below about 10^{-16} m^2. Table 6 shows that the permeability coefficients for water saturated materials are likely to lie below this value and hence will be crucial in determining the stress. The value of the permeability coefficient used as the typical value was 10^{-18} m^2, somewhat below the measured permeability coefficient for the reference backfill grout in the 100 % relative humidity conditioned state.

6.3 Behaviour in a Repository

The comparative performance of the cementitious materials studied in this work is summarised in Figure 12. As discussed above, the crucial parameters in determining the calculated level of tangential hoop stress at the void surface are the void radius and the permeability coefficient of the surrounding material. Figure 12 shows the calculated stress for permeability coefficients between 10^{-22} and 10^{-14} m^2 for voids of 0.02, 0.1 and 0.5 m radius using the typical values for the remaining parameters. The measured ranges of the permeability coefficients for the cementitious materials are also illustrated, plotted at stress values equal to the estimated tensile strength of each material based on one tenth of the compressive strength. If the tensile strength of the material at an appropriate permeability is exceeded by the calculated stress then the material is predicted to fail by cracking at the void.

Figure 12 indicates that the two backfill grouts can adequately disperse gas and hence will not fail. In contrast, the PFA/OPC-concrete and the BFS/OPC-grout appear to have insufficient permeability in the saturated state to prevent cracking. The simplicity of the model and the uncertainty in some of the parameters, in particular the permeability coefficients, Poisson's ratios and tensile strengths, require that these conclusions are tentative.

7 Conclusions

The gas permeability coefficients for generic repository construction materials have been determined for specimens in dry and in both partially and fully water saturated conditions. It has been shown that the permeability of the structural PFA/OPC-concrete is dependent on both gas type and average pressure under all conditions. The permeability coefficient is approximately independent of average pressure at pressures above about 1 MPa. These effects are attributable to

an additional component of gas flow caused by significant Knudsen flow at lower average pressures. The permeability coefficient is significantly reduced for water saturated conditions due to a reduction in the volume of porosity available for gas flow.

Gas flow in the two high porosity backfill materials is not significantly dependent on the average pressure in the range 100 kPa to 3 MPa. Some differences are observed for measurements carried out using helium and argon. The contribution of Knudsen flow to gas migration in these materials is small at the average pressures studied due to the generally larger pore size when compared with the structural concrete. The permeability coefficient is significantly reduced when the materials are water saturated, but it remains several orders of magnitude greater than that observed in the PFA/OPC-concrete. The BFS/OPC-grout, typical of the encapsulation materials placed within waste packages, has a similar permeability coefficient to those measured for the backfill grouts when dry but exhibits a significantly lower permeability, close to that of the concrete, when water saturated. Some dependence on average pressure is observed. The properties of this material may be affected by damage during drying.

The observed permeability coefficients for water saturated materials are all significantly greater than the permeability coefficient predicted by the solution-diffusion mechanism of gas migration. This may be due to the movement or displacement of the water within the pore structure. Such an effect would result in an increase in the permeability coefficient at higher applied pressures.

The presence of interfaces within the cementitious materials, such as construction joints and reinforcement bars, results in an increase in the permeability of the materials when water is present. No significant increase was observed in dry materials.

A simple model of the development of cracking in cementitious materials in repositories has been developed. The model identifies the gas permeability coefficient as a crucial parameter in determining the likelihood of cracking through gas generation in voids. Initial calculations indicate that the backfill grouts studied in this work should be able to release gas at a sufficient rate to avoid cracking.

Acknowledgements

References

1. Proceedings of joint NEA/CEC Workshop, "Sealing of Radioactive Waste Repositories", Paris (1989).

2. R.E. Cunningham and R.J.J. Williams, "Diffusion in gases and porous media", Plenum Press, New York (1980).

3. F.A.L. Dullien, "Porous media - Fluid transport and pore structure", Academic Press, New York (1979).

4. C.H. Geankoplis, "Mass transport phenomena", Holt, New York (1972).

5. C.N. Satterfield, "Mass transfer in heterogeneous catalysis", MIT Press, Cambridge, Massachusetts (1970).

6. R.E. Collins, "Flow of fluids through porous media", Renhold Pub. Co., New York (1960).

7. L.J. Klinkenberg, *Drilling and Production Practice* (1941), 200.

8. P.B. Bamforth, *Mag. Concrete Res.* **39** (1987), 3.

9. M. Knudsen, *Ann. Phys.* **28** (1909), 75.

10. J. Crank, "The mathematics of diffusion", Clarendon Press, Oxford (1956).

11. K.P. McCarty and E.A. Mason, *Phys. Fluids* **3** (1960), 908.

12. R.B. Evans III, G.M. Watson and E.A. Mason, *J. Chem. Phys.* **35** (1961), 2076.

13. S. Goto and D.M. Roy, *Cement Concrete Res.* **11** (1981), 575.

14. R.H. Mills, *Mat. Res. Soc. Symp. Vol. 85* (1987), 135.

15. G.R. Martin, *Mag. Concrete Res.* **38** (1986), 90.

16. J.G. Cabrera and C.J. Lynsdale, *Mag. Concrete Res.* **40** (1988), 177.

17. H. Grube and C.D. Lawrence, Proc. RILEM Seminar on "The Durability of Concrete Structures under Normal Outdoor Exposure", Hannover (1984).

18. H. Grube and C.D. Lawrence, Cembureau Draft report (1985).

19. J.W. Figg, *Mag. Concrete Res.* **25** (1973), 213.

20. L. Chou Chen and D.L. Katz, *ACI Journal* (1978), 673.

21. M. Daimon, T. Akiba and R. Kondo, *J. Am. Ceram. Soc.* **54** (1971), 423.

22. A.W. Harris, A. Atkinson, A.K. Nickerson and N.M. Everitt, Nirex Safety Study Report NSS-R125 (1988).

23. C.R. Wilding, private communication.

24. C.D. Lawrence, conference paper (1985).

25. K. Tuutti, in "Corrosion of steel in concrete", Swedish Cement and Concrete Research Institute, Stockholm (1982), 146.

26. M.V.J. Culot, H.G. Olson and K.J. Schiager, *Health Phys.* **30** (1976), 263.

27. R.F. Holub, R.F. Droullard, T.B. Borak, W.C. Inkret, J.G. Morse and J.F. Baxter, *Health Phys.* **49** (1985), 267.

28. C.L. Page, N.R. Short and A. El Tarras, *Cement Conc. Res.* **11** (1981), 395.

29. A. Atkinson and A.K. Nickerson, *J. Mater. Sci.* **19** (1984), 3068.

30. C.L. Page and P. Lambert, *J. Mater. Sci.* **22** (1987), 942.

31. A.W. Harris and A.K. Nickerson, Nirex Safety Study Report NSS-R189 (1989).

32. A.W. Harris, unpublished data.

33. A.W. Harris and A.K. Nickerson, Nirex Safety Study Report NSS-R215 (1990).

34. T. Roark and C. Young, "Formulas for stress and strain (5th Edition)", McGraw-Hill (1975).

List of Tables

12. Summary of the conclusions of the stress generation model. The variation in tangential hoop stress at the void surface for three different void radii is plotted against permeability coefficient. The estimated tensile strengths for the materials investigated in this work are also plotted against the range of the permeability coefficients. A material is considered to crack if the calculated stress exceeds the tensile strength, as shown by the regions labelled "pass" and "fail" (crack).

Material	Water-binder ratio	Aggregate-binder ratio	Total binder content / kg m^{-3}
SRPC-concrete	0.45	4.0	413
PFA/OPC-concrete	0.475	4.55	400
BFS/OPC-grout	0.4	0	1350

Table 1   Water-cement and aggregate-binder ratios and total binder content used in the manufacture of the experimental materials. Data for backfill grouts are unavailable. All ratios are by weight.

Material	Strength / MPa	Density / kg m^{-3}	Percentage Porosity		Average pore radius / μm
			Wt. loss	MIP	
SRPC-concrete	64.0	2478	13	-	-
PFA/OPC-concrete	61.0	2430	12	11	0.011
BFS/OPC-grout	32.0	1890	40	29	0.011
Preliminary grout	0.9	1460	66	56	0.70
Reference grout	6.0	1755	54	44	0.45

Table 2   Physical properties of the experimental materials. Average pore radius values obtained using mercury intrusion porosimetry (MIP).

Material	Dry		75 % RH		100 % RH	
	Wt.	GAV	Wt.	GAV	Wt.	GAV
PFA/OPC-concrete	14.3	2.9	1.2	-2.3	0	6.9
BFS/OPC-grout	44.4	23.1	2.0	3.8	0	3.7
Preliminary grout	66.3	67.2	56.0	-	35.9	42.6
Reference grout	55.1	54.9	25.1	33.4	11.4	12.7

Table 3   Fractional porosities obtained from the weight loss for each material during conditioning in the given relative humidity atmosphere (Wt.) and from the measurement of gas accessible volumes (GAV). Negative value is due to inaccuracy in the measurement

Average Pressure / 100kPa	$k / 10^{-17} m^2$	$D / 10^{-8} m^2s^{-1}$
1.00	1.66	3.32
1.25	1.40	3.26
1.55	1.18	3.74
1.75	1.08	2.50

Table 4   Calculated values of the hydrogen-argon inter-diffusion coefficient for the dry SRPC-concrete at the average pressures shown. The appropriate values of the argon permeability coefficient, derived from Figure 4, used in the calculation are also given.

Gas	Mean free path at 100 kPa / μm	k_∞ / 10^{-17} m^2	b / 100 kPa	
			Low pressure	High pressure
Hydrogen	0.194	4.9±1.1	1.9±1.1	-
Helium	0.305	5.2±0.9	1.9±0.8	0.9±1.0
Methane	0.086	4.6±1.6	0.3±0.3	-
Argon	0.110	2.4±0.3	1.6±0.3	2.6±3.7
Carbon Dioxide	0.070	1.9±0.2	0.5±0.2	5.6±3.4

Table 5 Results of the measurements of gas flow in dry PFA/OPC-concrete using varying average pressure. Data given are the means of the best-fit values for the Klinkenberg equation. Low pressure data obtained for average pressures in the range 0 to 200 kPa. High pressure data obtained for average pressures in the range 0 to 7.5 MPa. Quoted errors are standard errors.

Material	Dry		100 % Relative Humidity	
	Helium	Argon	Helium	Argon
SRPC-concrete	-	2×10^{-17}	-	-
PFA-concrete	6×10^{-17}	3×10^{-17}	7×10^{-20}	10^{-21}
BFS-grout	5×10^{-16}	4×10^{-16}	4×10^{-19}	10^{-21}
Prelim. grout	2×10^{-14}	10^{-14}	2×10^{-16}	4×10^{-17}
Reference grout	3×10^{-15}	2×10^{-15}	7×10^{-17}	4×10^{-17}

Table 6 Measured permeability coefficients for a constant average pressure of 100 kPa in the experimental materials. All data are expressed as k / m^2.

Material	Dry	100 % Relative Humidity
SRPC-concrete	$(3.8\pm0.1)\times10^{-18}$	-
PFA/OPC-concrete	$(3.7\pm0.6)\times10^{-17}$	-
BFS/OPC-grout	$(5.3\pm1.0)\times10^{-16}$	$(5.9\pm0.4)\times10^{-18}$
Preliminary grout	$(4.4\pm1.1)\times10^{-14}$	$(4.4\pm0.8)\times10^{-16}$
Reference grout	$(4.4\pm1.1)\times10^{-16}$	$(4.6\pm5.0)\times10^{-16}$

Table 7   Measured values of the infinite pressure permeability coefficient. Data for the dry conditioned specimens obtained for pressures in the range 0 to 100 kPa only. Quoted errors are standard errors. All data are expressed as $k\,/\,m^2$.

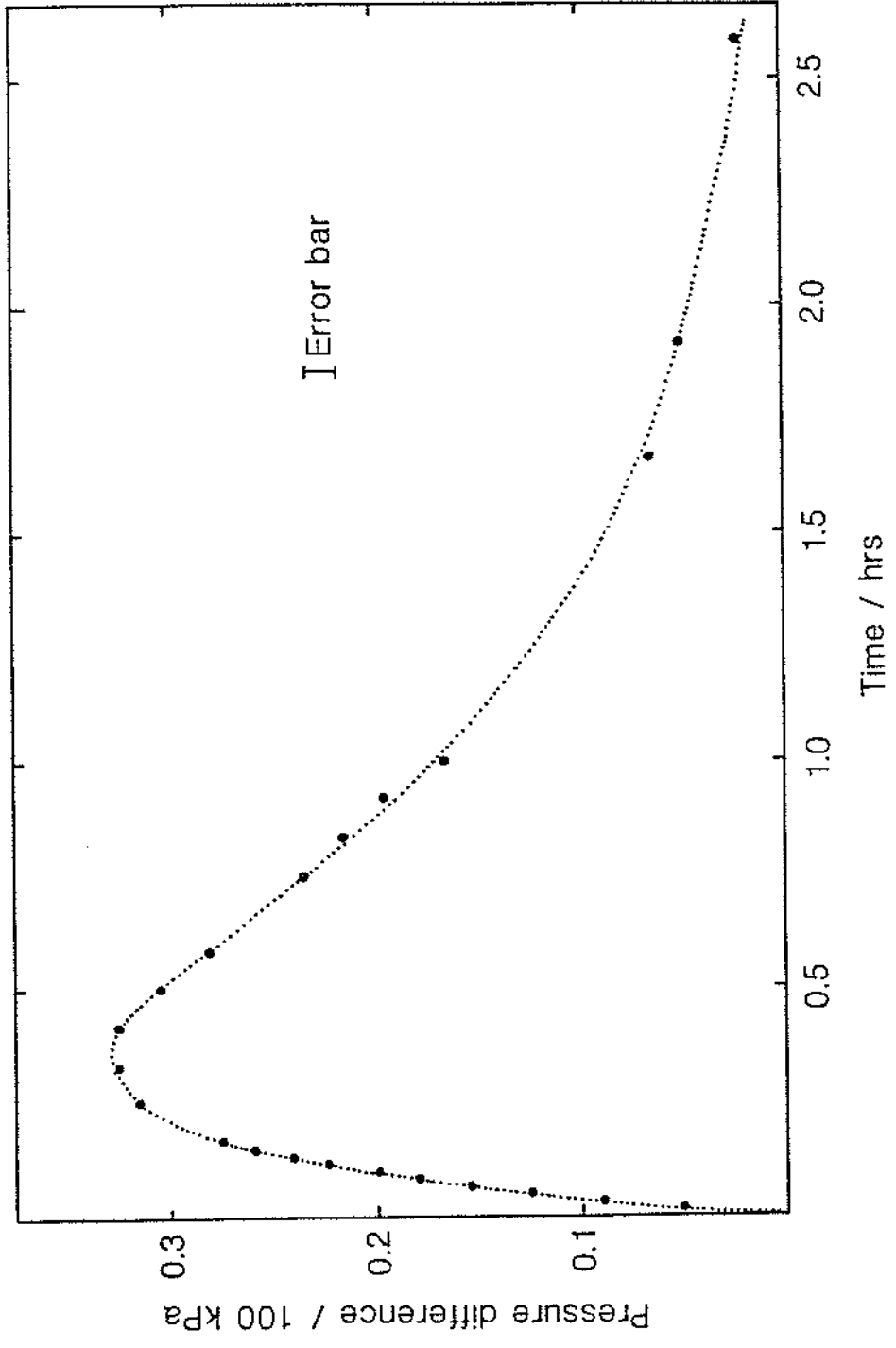| Material	Low Pressure (100 kPa)		High Pressure (>100 kPa)	
	Helium	Argon	Helium	Argon
PFA/OPC-concrete	1.9±0.8	1.6±0.3	0.9±1.0	2.6±3.7
BFS/OPC-grout	0.5±0.3	-(0.3±0.1)	1.2±0.6	-(1.8±3.7)
Preliminary grout	-(0.4±0.2)	-(0.8±0.2)	2.3±0.3	1.1±0.2
Reference grout	20.6±9.5	6.0±1.9	2.2±0.7	-(3.7±1.9)

Table 8   Measured values of the Klinkenberg constant for materials in the dry condition obtained using varying average pressure experiments. The low pressure data are corrected by a factor of 1.13 to allow for differing areas. Where quoted the errors are standard errors. All data are expressed as $b\,/\,10^5$ Pa.

			Rebar in Concrete	Joint in Backfill
k measured at 100 kPa	Dry	Helium	2×10^{-16}	-
		Argon	10^{-16}	4×10^{-14}
	100 % RH	Helium	5×10^{-21}	3×10^{-15}
		Argon	6×10^{-21}	2×10^{-15}
Infinite Pressure Permeability	Dry		$(2.0 \pm 0.7) \times 10^{-16}$	2.19×10^{-13}
	100 % RH		1.08×10^{-19}	$(4.4 \pm 1.9) \times 10^{-15}$

Table 9   Measured values of the permeability coefficients for the flawed specimens. The constant average pressure data were obtained from experiments at an average pressure of 100 kPa. Where quoted, errors are standard errors. All data are expressed as k / m^2.

50 mm

PLAN

4mm ⌀

4mm ⌀

300 mm

100

FRONT ELEVATION

MESH

50 mm

TYPICAL
SLICE
POSITION

SIDE ELEVATION

Fig 2.

Fig. 3

Time / min

Hydrogen conc / %

fig 4

fig 6

PERMEABILITY COEFFICIENT /$10^{-19}m^2$

PERMEABILITY COEFFICIENT/ $10^{-19}m^2$

PERMEABILITY COEFFICIENT / $10^{-20}m^2$

DRY

75% RH

100% RH

Fig 7

FIG 8

PERMEABILITY COEFFICIENT / $10^{-13} m^2$

AVERAGE PRESSURE / 100 kPa

Fig. 12